# Geometry and Simulation Results for a Gas Turbine Representative of the Energy Efficient Engine (EEE)

*Russell W. Claus*
*Glenn Research Center, Cleveland, Ohio*

*Tim Beach*
*Coyote Hollow Consulting, LLC, Walton Hills, Ohio*

*Mark Turner and Kiran Siddappaji*
*University of Cincinnati, Cincinnati, Ohio*

*Eric S. Hendricks*
*Glenn Research Center, Cleveland, Ohio*

# NASA STI Program . . . in Profile

Since its founding, NASA has been dedicated to the advancement of aeronautics and space science. The NASA Scientific and Technical Information (STI) Program plays a key part in helping NASA maintain this important role.

The NASA STI Program operates under the auspices of the Agency Chief Information Officer. It collects, organizes, provides for archiving, and disseminates NASA's STI. The NASA STI Program provides access to the NASA Technical Report Server—Registered (NTRS Reg) and NASA Technical Report Server—Public (NTRS)  thus providing one of the largest collections of aeronautical and space science STI in the world. Results are published in both non-NASA channels and by NASA in the NASA STI Report Series, which includes the following report types:

- TECHNICAL PUBLICATION. Reports of completed research or a major significant phase of research that present the results of NASA programs and include extensive data or theoretical analysis. Includes compilations of significant scientific and technical data and information deemed to be of continuing reference value. NASA counter-part of peer-reviewed formal professional papers, but has less stringent limitations on manuscript length and extent of graphic presentations.

- TECHNICAL MEMORANDUM. Scientific and technical findings that are preliminary or of specialized interest, e.g., "quick-release" reports, working papers, and bibliographies that contain minimal annotation. Does not contain extensive analysis.

- CONTRACTOR REPORT. Scientific and technical findings by NASA-sponsored contractors and grantees.

- CONFERENCE PUBLICATION. Collected papers from scientific and technical conferences, symposia, seminars, or other meetings sponsored or co-sponsored by NASA.

- SPECIAL PUBLICATION. Scientific, technical, or historical information from NASA programs, projects, and missions, often concerned with subjects having substantial public interest.

- TECHNICAL TRANSLATION. English-language translations of foreign scientific and technical material pertinent to NASA's mission.

For more information about the NASA STI program, see the following:

- Access the NASA STI program home page at http://www.sti.nasa.gov

- E-mail your question to help@sti.nasa.gov

- Fax your question to the NASA STI Information Desk at 757-864-6500

- Telephone the NASA STI Information Desk at 757-864-9658

- Write to:
  NASA STI Program
  Mail Stop 148
  NASA Langley Research Center
  Hampton, VA 23681-2199
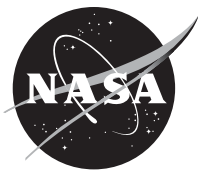
NASA/TM—2015-218408

# Geometry and Simulation Results for a Gas Turbine Representative of the Energy Efficient Engine (EEE)

*Russell W. Claus*
*Glenn Research Center, Cleveland, Ohio*

*Tim Beach*
*Coyote Hollow Consulting, LLC, Walton Hills, Ohio*

*Mark Turner and Kiran Siddappaji*
*University of Cincinnati, Cincinnati, Ohio*

*Eric S. Hendricks*
*Glenn Research Center, Cleveland, Ohio*

National Aeronautics and
Space Administration

Glenn Research Center
Cleveland, Ohio 44135

February 2015

# Acknowledgments

# Geometry and Simulation Results for a Gas Turbine Representative of the Energy Efficient Engine (EEE)

Russell W. Claus
National Aeronautics and Space Administration
Glenn Research Center
Cleveland, Ohio 44135

Tim Beach
Coyote Hollow Consulting, LLC
Walton Hills, Ohio 44146

Mark Turner and Kiran Siddappaji
University of Cincinnati
Cincinnati, Ohio 45220

Eric S. Hendricks
National Aeronautics and Space Administration
Glenn Research Center
Cleveland, Ohio 44135

## Abstract

This paper describes the geometry and simulation results of a gas-turbine engine based on the original EEE engine developed in the 1980s. While the EEE engine was never in production, the technology developed during the program underpins many of the current generation of gas turbine engines. This geometry is being explored as a potential multi-stage turbomachinery test case that may be used to develop technology for virtual full-engine simulation. Simulation results were used to test the validity of each component geometry representation. Results are compared to a zero-dimensional engine model developed from experimental data. The geometry is captured in a series of Initial Graphical Exchange Specification (IGES) files and is available on a supplemental DVD to this report.

## Nomenclature

| | |
|------|------|
| BPR | By Pass Ratio |
| CAD | Computer Aided Design |
| EEE | Energy Efficient Engine |
| HPC | High Pressure Compressor |
| HPT | High Pressure Turbine |
| ICLS | Integrated Core Low Spool |
| IGES | Initial Graphical Exchange Specification |
| LPC | Low Pressure Compressor |
| LPT | Low Pressure Turbine |
| Nc | Corrected rotational speed |
| NLH | Non-Linear Harmonic |
| NPSS | Numerical Propulsion System Simulator |

## 1.0    Introduction

NPSS (Numerical Propulsion System Simulator) was a NASA program created in the early 1990s to build a virtual engine simulation capability (Ref. 1). Leveraging advanced computing technologies, its

goal was to develop a framework that enabled reduced development timeframes based on virtual engine simulation. The project developed research efforts that explored multi-fidelity, multidiscipline models of engine systems to baseline computational accuracies and address fundamental questions exploring the practicality of the technique (Ref. 2). Today, NPSS is used as a zero-dimensional engine model simulation environment supporting the development of many new propulsion systems.

Beyond a few demonstrations (Refs. 2, 3, and 4) of full engine simulations, the practical application of NPSS remains as a zero-dimensional cycle model. Until recently, a full, three-dimensional simulation of a gas turbine engine was not a practical capability for any engineering organization. Today, many advances make full-engine simulations practical. First, computational resources for these simulations may be demanding but the advance of chip and software technology has greatly mitigated this challenge. Second, many engine component simulations employ proprietary codes and models which limit the utility of the simulation. Commercial codes, while not fully comprehensive, are making significant progress to reduce this limitation. A third limitation is the availability of geometry to test and improve component codes in a full system environment. Previous studies have used proprietary geometries that could not be further disseminated.

This report publishes geometry files from a series of reports (Refs. 5, 6, and 7) and the original Compter Aided Design (CAD) derived drawings. The geometry is captured in a series of Initial Graphical Exchange Specification (IGES) files. Some of these IGES files trace to the original CAD drawings for the EEE turbomachinery. Some of the files (specifically for the HPC) were not created from the original CAD drawings, but were recreated from the data in the NASA contractor report (Ref. 5). The original CAD-based files were used in a series of simulations by Hall (Ref. 4, 8, and 9).

A series of three-dimensional numerical simulations were conducted to validate the geometry. The High Pressure Compressor (HPC) was the most challenging component to simulate and the geometry from the two different sources provided significantly different results. A recommendation for component simulations is provided based on the calculations for each turbomachinery component of the engine. It is shown that these results, which should be considered preliminary, may be adequate to assemble into a full gas-turbine simulation. Additionally, it is hoped that the geometries can be used as multi-stage benchmark testcases to further the development of new models and simulation techniques.

## 2.0    EEE Geometry

In the 1980s, NASA funded the Energy Efficient Engine program to demonstrate fuel efficient designs for the next generation of transport aircraft. New low-emission combustor designs were tested to meet emissions goals. For the turbomachinery, the primary focus was to meet a 12 percent reduction in installed specific fuel consumption. Both Pratt & Whitney and General Electric (GE) were awarded development contracts. The GE design was carried forward into Integrated Core/Low Spool (ICLS) testing (Ref. 10). This full-system, integrated testing provides a full-engine dataset that was not available with the Pratt and Whitney design. The GE version was therefore selected for this study. Figure 1 illustrates the GE EEE design.

At the start of the NPSS program, one of the goals was to create a geometry database that could be freely distributed to participating stake-holders. A team of NASA engineers and contractors worked with the original CAD files (obtained from GE) and created a series of IGES surfaces representing the flow path and blade shapes for the EEE turbomachinery. These geometry files were used in a series of engine component and full system calculations by Hall (Ref. 4).

The overall EEE turbomachinery geometry, is illustrated in Figure 2. This figure displays the various engine components and indicates that each blade shape is represented by a series of cross-sectional views. The fan is captured by approximately 20 cross-sections, while the LPT displays only 5 cross-sections. These cross-sections are stacked radially and the turning between each cross-section can be fairly large, as is seen in Figure 3. IGES surfaces were constructed to closely match the cross-sections, but the significant variation between cross-sections made a perfect fit challenging. The variation between the cross-sections and the IGES surface may be a source of potential error in the blade shape representations.
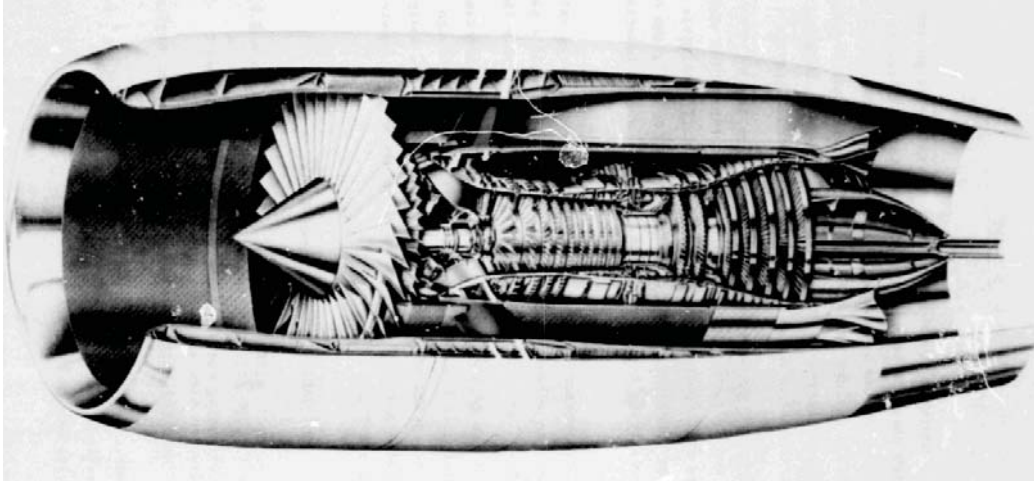
Figure 1.—Energy Efficient Engine developed by General Electric.
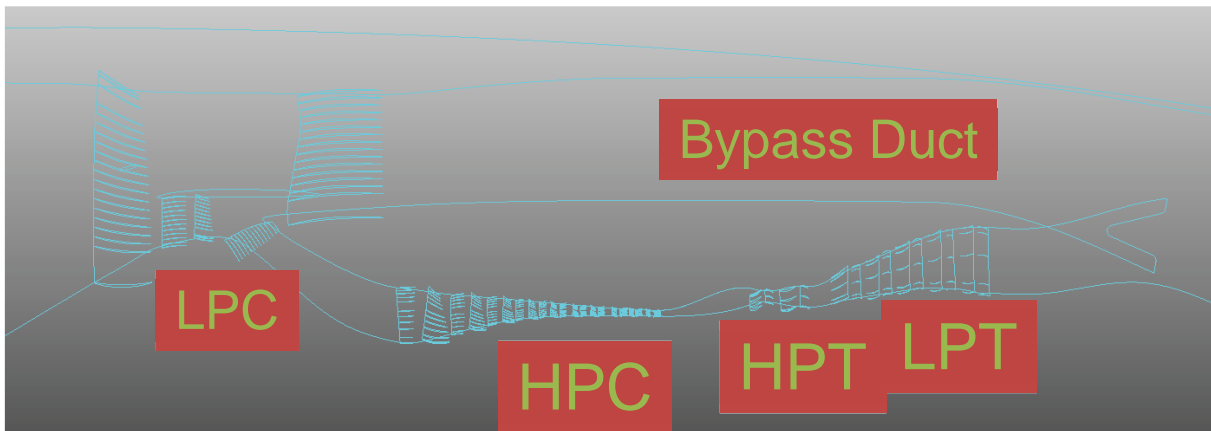


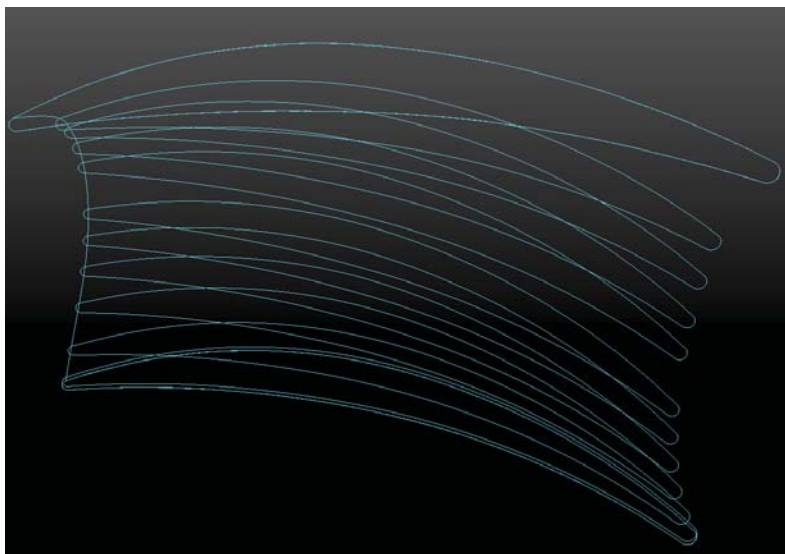Figure 2.—Engine component geometry illustrated as a series of blade cross-sections.



Figure 3.—Three-dimensional, perspective view of a stator blade showing the cross-sectional stacking and the radial shape variation.

Geometry files published with this report are organized as listed in Appendix A. Each component series of blade shapes is organized into a separate directory such as HPC, HPT, LPT or LPC. End walls or the limits of the flow domain can be extracted from the overall geometry file: "EEE_engine_all.igs" or "hub and casing" curves are provided in each component subdirectory. Blade counts are captured in Appendix B. In ensemble, these files provide much of the basic information needed for turbomachinery simulation. Information of the film-cooling or bleed can be extracted from Holloway (Ref. 6), Timko (Ref. 7) and Bridgeman (Ref. 11).

At the top directory, the "EEE_engine_all.igs" file is stored along with symmetric and unsymmetrical elements. The original tar file used to store all this data is also stored in the root directory. This original tar file stored the file information in a version-control application that mangled these file labels. However, for this publication, the file names have been repaired based on information contained within each IGES file.

The quarter stage booster and fan are included in the LPC directory. A series of curves provide information on the splitter and part-span shroud.

Two directories for the HPC can be seen. The first labeled "HPC" is derived from the same source as all the other geometry files (GE). The directory labeled "HPC-CR16558 Derived" was developed by Turner and Siddappaji at the University of Cincinnati, using only information in Holloway (Ref. 6). This reference noted that a variety of blade shapes were used in the HPC (NACA series, Circular Arcs and others), but it was unclear which blade shape was used for any particular rotor or stator. For this reason, the blade thickness was determined from a general area rule. These blade shapes display significant differences between the GE original CAD shapes and the IGES representations from Holloway (Ref. 6). Appendix C illustrates the difference in leading and trailing edge profiles between the two different series of files. Large discrepancies are seen in the rotors 8, 9 and 10 and several stators.

The EEE HPC was developed in the 1980s with two different "builds" or test articles. The second build was developed to improve on the original geometry documented in Holloway (Ref. 6). Holloway represents the first build while the geometry GE CAD shapes represent the second build. The impact of this variation will be discussed in Section 3.0, Engine System Performance.

HPT and LPT directories are organized as the other components.

## 2.1    Open Data Sources for the EEE Geometry

As has been noted in the previous section, the blade shapes for each component of the EEE can be largely reconstructed from the NASA Contractor Reports (Refs. 6, 7, 10, and 11). HPC shapes were extracted from Holloway (Ref. 6) for the first build of the EEE HPC. HPT blade coordinates were listed in Appendix A of Timko (Ref. 7). Scale drawings of the blade cross-section at three radial locations (hub, pitch and tip) are also available in this reference. Figure 1 in Timko provided detailed dimensions for the flow path.  The LPT blade shapes were documented in Bridgeman (Ref. 11) through scale drawings of Figures 10 to 19. The flow path was documented in Figure 9. While these sources are not as reliable as the actual CAD representations, they do provide adequate information to analyze highly similar systems.

## 3.0    Engine System Performance

This section explores some numerical simulations of the EEE turbomachinery geometry documented in Section 2.0. New simulation results are placed in context by comparing with previous efforts (Ref. 4). Previous efforts were based on computer simulation technology of the 1990s with relatively course mesh resolution, constant gamma and a mixing plane treatment of the rotor / stator interaction. Modern CFD tools provide more options for numerical accuracy, much finer mesh resolution, and an improved treatment of the rotor / stator interaction using a Non-Linear Harmonic (NLH) method (Ref. 12). It was of interest to see if these improvements resulted in better system performance.

Numerical simulations of the rotating turbomachinery involved solving the Reynolds's Averaged Navier-Stokes equations using the Numeca FINE/Turbo code suite (Ref. 12). This software has a fully

integrated suite of tools that enables rapid mesh generation, domain decomposition, flow solving, and visualization. The mesh generation can be controlled through a series of utilities that tailor the grid topology and optimization to the application-specific geometry. Typically, the defaults for the mesh generation provide good mesh characteristics; however, adjustments were made using available manual controls. FINE/Turbo employs a variety of possible rotor/stator interface techniques, turbulence models, and differencing techniques. In this study, the steady-state options were used, including the Mixing Plane approximation, the Spalart-Almos turbulence model, and Flux Difference Splitting (second order upwind) with Min Mod limiters. Some calculations of the HPC were made using the NLH method.

Hall's simulation results (Ref. 4) (representative of early modeling efforts) can be seen in Table 1 for the simulated EEE system values and a cycle model. This cycle model was matched to the experimental engine tests(Ref. 10) by Owen and documented in Hall (Ref. 4). As can be seen in Table 1, the turbines exhibit poor corrected mass flow, pressure ratios, and efficiencies. However, the HPC is very well matched and the other compression components are all within a few percent of the cycle model results. Given the state of mesh resolution, constant gamma and model complexity in this study, the overall predictive accuracy is surprisingly good. However, if all these component simulations were fully coupled to the 0–D NPSS model, it seems likely that the predicted engine performance would not closely resemble the EEE.

With the recent advances in simulation capabilities, many of the EEE engine turbomachinery components have been analyzed again to better predict performance. Table 2 illustrates the component performance calculated using Fine/Turbo in these simulations for much of the EEE engine turbomachinery. The Fan/LPC component is not displayed as calculations of this component were not performed. Overall, the efficiency of each component is fairly good, with the exception of the LPT. The LPT displays a –3 percent performance variance. This level of inaccuracy may be due to a large number of factors, including poor development of the geometry, and model/mesh limitations. The good agreement seen in the HPT may be fortuitous as film cooling was not included and would likely alter the indicated performance.

All calculations were performed with smooth hub and casing surfaces, whereas, a more realistic representation would include hub leakages, turbine blade film cooling, secondary flow paths, and a capturing of the "button" geometry for the variable angle stators in the HPC. These calculations employed a mixing plane assumption for the rotor / stator interaction plane and better models may have improved the calculated results. The following sections discuss details of each component simulation.

TABLE 1.—ENGINE SYSTEM PERFORMANCE RESULTS OF
HALL'S SIMULATIONS COMPARED WITH A 0–D CYCLE
MODEL BASELINED TO EXPERIMENTAL DATA

|  | Wc, % | PR, % | Efficiency, % |
|---|---|---|---|
| FAN | 3.23 | −1.80 | 1.16 |
| LPC | 0.59 | −1.67 | 1.99 |
| HPC | −0.29 | −0.22 | −0.30 |
| HPT | −6.17 | −6.11 | −2.88 |
| LPT | 10.11 | 11.49 | −1.32 |

TABLE 2.—COMPONENT SIMULATION VARIANCES
FROM THE BASELINE 0–D NPSS MODEL

| Component | W, % | PR, % | Efficiency, % |
|---|---|---|---|
| HPC | 3.45 | −0.68 | −0.89 |
| HPT | 6.64 | 1.55 | 0.32 |
| LPT | 8.32 | 2.32 | −3.00 |

## 3.1    High Pressure Compressor (HPC)

The HPC was the most difficult component to simulate as might be expected from the high pressure-ratio compression performed by the system. The HPC, nominally, could perform at a pressure ratio of 25 although the calculations performed here were limited to about 23. As was reported earlier, the blade shapes directly traceable to GE CAD drawings had significant differences from the shapes developed from Holloway (Ref. 6). All calculations performed using the GE CAD geometry did not converge. The calculations reported here used the shapes derived from Holloway (Ref. 6).

Tip clearances were illustrated in Holloway (Ref. 6). Figure 4 is recreated from Figure 62 of this reference. The estimated line was presumably calculated using measured temperatures and pressure from rig testing. Two probe tip-clearance measurement locations were documented and match well within the estimated range of value.

The baseline HPC calculation seen in Table 2 was performed using the mixing plane assumption with flux-difference splitting of the momentum equations. The use of flux-difference splitting was important as central differencing resulted in reduced efficiencies and ultimately, the central difference calculation would not converge. The flux-differencing splitting, combined with mixing-plane, resulted in the work loading seen in Figure 5. This figure illustrates the percent of the total temperature rise occurring across each stage. The first two stages are highly loaded with the remaining stages experiencing between 9 and 10 percent temperature rise.

All HPC calculations were performed using 15,462,827 mesh nodes, with rotor blades typically employing about 1 million nodes and the stators at a lower level of resolutions of about 600K nodes.
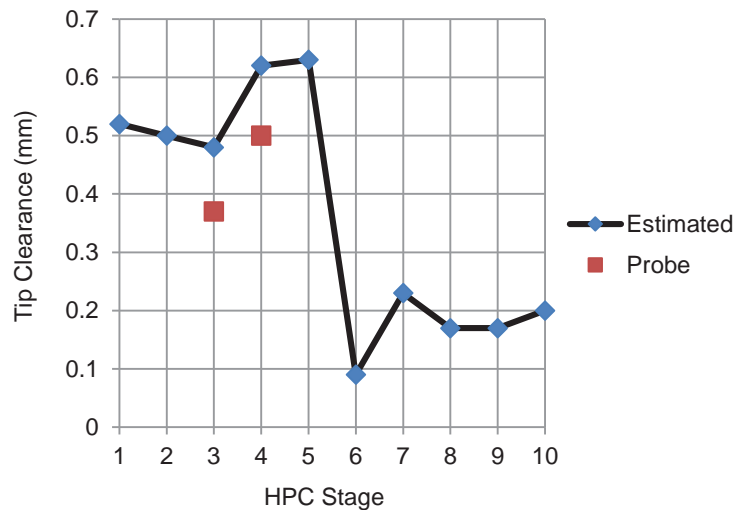


Figure 4.—HPC tip clearances as estimated and measured from Holloway.
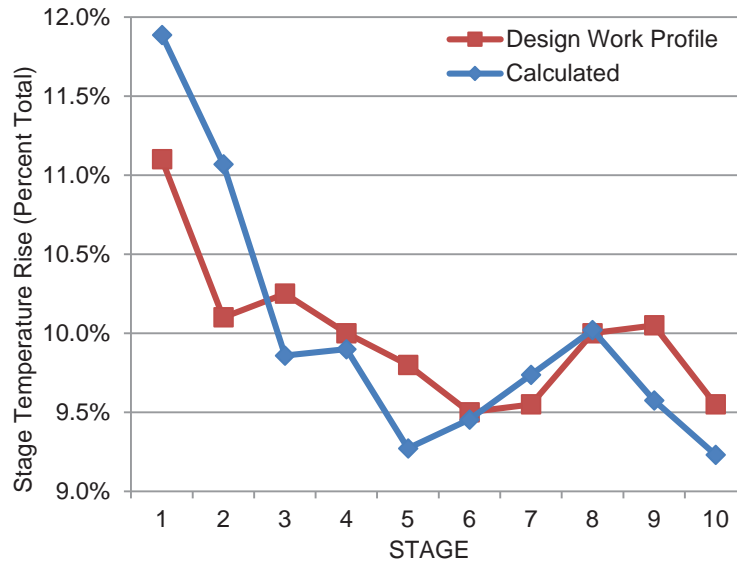
Figure 5.—Stage distribution of temperature rise (work loading) for the design and numerically calculated results.

## 3.2    High Pressure Turbine (HPT)

The HPT calculations were performed using Fine-Turbo with 3,828,020 nodes, central differencing, and with the mixing plane model for rotor / stator interactions. This simulation employed smooth sidewalls and no cooling bleed. The cooling bleed and sidewall treatment are obvious areas for improvement in this calculation. Despite these limitations the system performance is well predicted.

Nominal tip clearance was documented by Timko (Ref. 7) as 41 mm.

From Hall (Ref. 4): "GE engineers familiar with the actual test rig and EEE engine geometry recommended a one degree (open) reset of the LP turbine first stage vane." This reset is maintained in these calculations.

## 3.3    Low Pressure Turbine (LPT)

The LPT calculation was performed with 12,410,092 nodes, central differencing and the mixing plane model. The calculated efficiency of 89.7 percent is lower that the cycle results, but this value is reasonable considering the limitations on the calculation. The boundary layer transition may be an area requiring further study / variation and, as with the HPT, bleed and sidewalls need to be improved. In general, the computed results are promising, but further study is suggested.

## 3.4    Summary

Overall, the component performance results suggest that a full coupling of the high-fidelity simulations with a 0D cycle simulation may be possible. Most component results are a fair match with system data. Much more simulation testing would be required to quantify the level of uncertainty, but the geometry provided by this report is certainly a good starting point for further refinement of the geometry and analysis features.

```
      MN      alt    dTamb        W        Fg        Fn       SFC      Fuel       WAR       OPR
   0.800   35000.0    18.00    524.5   21262.2    8351.3    0.5366   4480.99    0.0000    36.279

            INPUT FLOW
                           Tt        Pt        Ps         W        Wc        MN      Aphy        ht        Ts       FAR      gamt
Input_StrmTube  >      464.50     5.292     3.458    522.12   1372.12    0.8000    4170.2    111.19    411.85    0.0000   1.40010
Input_EngInl    >      464.50     5.292     3.860    522.12   1372.12    0.6868    4416.9    111.19    424.49    0.0000   1.40010
Input_FanSplit  >      464.50     5.292     4.115    522.12   1372.12    0.6105    4703.7    111.19    432.29    0.0000   1.40010
Input_FanTip    >      464.50     5.292     4.110    404.29   1062.47    0.6105    3646.5    111.19    432.29    0.0000   1.40010
Input_FanTipExtD>      543.01     8.625     7.524    404.29    704.82    0.4460    2996.3    130.03    522.25    0.0000   1.39973
Input_LPC       >      464.50     5.292     4.110    117.83    309.65    0.6105    1062.7    111.19    432.29    0.0000   1.40010
Input_LPCSplit  >      544.51     8.746     7.449    117.83    202.85    0.4844     810.5    130.38    520.11    0.0000   1.39973
Input_LPCTipDct >      544.51     8.746     7.439     53.83     92.68    0.4844     370.8    130.38    520.12    0.0000   1.39973
Input_LPCMix_I1 >      543.01     8.625     7.425    404.29    704.82    0.4676    2890.6    130.03    520.28    0.0000   1.39973
Input_LPCMix_I2 >      544.51     8.746     7.425     53.83     92.68    0.4893     367.6    130.38    519.64    0.0000   1.39973
Input_BypDct    >      543.19     8.639     7.426    458.12    797.52    0.4700    3258.2    130.07    520.22    0.0000   1.39973
Input_BypBld    >      543.19     8.278     0.000    458.12    832.31    0.0000       0.0    130.07      0.00    0.0000   1.39973
Input_HPCInlDct >      544.51     8.746     8.451     63.99    110.17    0.2220     862.1    130.38    539.20    0.0000   1.39973
Input_HPCInlBld >      544.51     8.746     7.774     63.99    110.17    0.4138     496.8    130.38    526.49    0.0000   1.39973
Input_HPC       >      544.51     8.746     7.774     63.99    110.17    0.4138     496.8    130.38    526.49    0.0000   1.39973
Input_HPCExtBld >     1431.19   191.987   183.597     61.85      7.86    0.2576      54.4    351.36   1414.53    0.0000   1.35446
Input_Brn       >     1431.19   191.987   185.751     53.66      6.82    0.2213      54.4    351.36   1418.87    0.0000   1.35446
Input_HPTInlBld >     2852.78   182.387     0.000     54.91     10.38    0.0000       0.0    774.14      0.00    0.0232   1.28458
HPT1Rcool       >     1431.19    36.881     0.000      3.41      2.26    0.0000       0.0    351.36      0.00    0.0000   1.35446
HPT2Vcool       >     1174.30    36.881     0.000      1.25      0.75    0.0000       0.0    285.07      0.00    0.0000   1.37012
Input_HPT       >     2749.02   182.387     0.000     59.68     11.07    0.0000       0.0    740.33      0.00    0.0213   1.28883
Input_LPTInlBld >     1919.47    36.881     0.000     64.34     49.32    0.0000       0.0    493.87      0.00    0.0197   1.31737
Input_LPT       >     1911.97    36.881     0.000     64.92     49.67    0.0000       0.0    491.64      0.00    0.0195   1.31778
Input_LPTExtDct >     1361.87     8.228     7.660     64.92    187.91    0.3274    1050.7    339.50   1337.08    0.0195   1.34503
Input_MainMix_I1>      543.19     8.278     7.016    458.12    832.31    0.4919    3288.4    130.07    518.13    0.0000   1.39973
Input_MainMix_I2>     1361.87     8.228     7.016     64.92    187.91    0.4913     755.4    339.50    518.24    0.0195   1.34503
Input_Nozz      >      650.48     8.211     6.881    523.05   1048.38    0.5094    4043.8    156.06    618.64    0.0024   1.39636
Input_NozzSnk   >      650.48     8.211     4.345    523.05   1048.38    1.0000    3053.3    156.06    542.53    0.0024   1.39636
LPTcoolOB       >     1013.95    61.699     0.000      0.31      0.10    0.0000       0.0    244.74      0.00    0.0000   1.38003
OvrBrd          >     1013.95    61.699     0.000      0.31      0.10    0.0000       0.0    244.74      0.00    0.0000   1.38003


         INLETS                                                      COMPRESSORS & TURBINES
               eRam        Afs       Fram                                    Wc        PR        TR    efPoly       eff      Nc|Np        pwr
StrmTube     1.0000    4170.24    12910.9               FanTip        1062.47     1.630    1.1690    0.8994    0.8936   3590.503   -10774.9
                                                        LPC            309.65     1.653    1.1722    0.9089    0.9033   3590.503    -3200.0
         DUCTS                                          HPC            110.17    21.951    2.6284    0.8865    0.8332  12086.703   -19755.0
              dPqP       MNin       Aphy                HPT             11.07     4.945    1.4024    0.9128    0.9270      236.2    19755.0
EngInl     0.00000     0.6868    4416.90               LPT             49.67     4.483    1.4039    0.9100    0.9247       77.7    13974.9
FanTipExt> 0.00000     0.4460    2996.30
LPCTipDct  0.00000     0.4844     370.82                MAP POINTS - COMPRESSORS & TURBINES
BypDct     0.04180     0.4700    3258.19                             WcMap     PRmap                       effMap       NcMap     R||parm
HPCInlDct  0.00000     0.2220     862.10               FanTip        1308.18     1.737                     0.8397      99.726      2.0536
LPTExtDct  0.00000     0.3274    1050.70               LPC            254.94     1.689                     0.8644      99.726      1.6079
                                                        HPC            112.29    30.923                     0.8013     100.208      1.1177
         SPLITTERS                                     HPT             15.77     4.799                     0.9213      99.137     76.0000
               BPR      dP/P1      dP/P2                LPT             15.78     4.732                     0.9210      98.394     76.0000
FanSplit   3.43125     0.0000     0.0000
LPCSplit   0.84122     0.0000     0.0000                ADDERS AND SCALARS
                                                                    s_WcAud   a_WcAud                               s_effAud   a_effAud
         MIXERS                                        FanTip         1.0000    0.0000                                1.0000     0.0000
              %mix        MN1        MN2        A1        A2       Ps1       Ps2     LPC            1.0000    0.0000                                1.0000     0.0000
LPCMix      1.00      0.468      0.489    2890.6    367.6     7.425     7.425     HPC            1.0000    0.0000                                1.0000     0.0000
MainMix     1.00      0.492      0.491    3288.4    755.4     7.016     7.016                  s_WpAud   a_WpAud    s_PRaud   a_PRaud   s_effAud   a_effAud
                                                        HPT            1.0000    0.0000     1.0000    0.0000     1.0000     0.0000
                                                        LPT            1.0000    0.0000     1.0000    0.0000     1.0000     0.0000

         SHAFTS                                         BLEEDS
             Nmech      trqIn     trqNet      pwrIn       HPX      dNqdt                              Wb/Win    dhb/dh    dPb/dP        Tt        ht
LPShaft    3397.8    21601.3    -0.0058    13974.9      0.00      -0.00     HPT2Vcool  HPC.HPT2Vcool    0.0195    0.7000    0.4953   1174.30    285.07
HPShaft   12384.1     8378.1     0.0026    19755.0      0.00       0.00     LPTcool    HPC.LPTcool      0.0091    0.5175    0.2890   1013.95    244.74
```

Figure 6.—Typical EEE engine system model output at cruise conditions.

## 4.0　EEE Engine Cycle

A 0–D representation of the ICLS engine was developed to support the simulations of Hall (Ref. 4). A typical output for cruise is illustrated in Figure 6. The complete NPSS model is included in accompanying compact disk.  This model may be helpful to future efforts building a fully-coupled engine simulation.

## 5.0　Summary

The intent of this paper was to document the EEE geometry that may provide a baseline for testing full-engine simulation techniques. It appears highly likely that some of the geometry provided here may not be an exact representation of the hot, operating geometry for all components. The blade shapes received from GE did not contain blade surfaces, and the NURBS representations created for the blades may have flaws. Simulation results indicate reasonable component performance, but the accuracy is still subject to a variety of uncertainties. There is a great need to add detailed hub leakages models, variable stator "button" geometries, film cooling and end wall flows. The openly published contractor reports provide much of the information needed to further refine this geometry. The refined simulations might result in significantly different performance.

# Appendix A.—Supplemental Information

Table 3 provides a listing of the files contained on the supplemental DVD available with this report.

TABLE 3.—LISTING OF FILES BY FOLDER CONTAINED IN SUPPLEMENTAL DVD

| File Name | Date Modified | Size (bytes) |
|---|---|---|
| Directory: \EEE | | |
| assem.igs | 12/12/2012 | 28,436,480 |
| directory.txt | 12/19/2012 | 0 |
| eee.tar.gz | 12/12/2012 | 14,202,965 |
| EEE_3d_sym.igs | 12/12/2012 | 426,465 |
| EEE_3d_uns.igs | 12/12/2012 | 9,596,232 |
| EEE_engine_all.igs | 12/12/2012 | 8,736,255 |
| HPC (Folder) | 12/19/2012 | |
| HPC-CR16558 Derived (Folder) | 12/19/2012 | |
| HPT (Folder) | 12/19/2012 | |
| LPC (Folder) | 12/19/2012 | |
| LPT (Folder) | 12/19/2012 | |
| Directory: \EEE\HPC | | |
| case.igs | 11/30/2009 | 41,310 |
| compr_igv.igs | 12/12/2012 | 194,319 |
| compr_rotor1.igs | 12/12/2012 | 275,400 |
| compr_rotor10.igs | 12/12/2012 | 187,353 |
| compr_rotor2.igs | 12/12/2012 | 275,886 |
| compr_rotor3.igs | 12/12/2012 | 249,804 |
| compr_rotor4.igs | 12/12/2012 | 241,380 |
| compr_rotor5.igs | 12/12/2012 | 241,461 |
| compr_rotor6.igs | 12/12/2012 | 219,510 |
| compr_rotor7.igs | 12/13/2012 | 222,426 |
| compr_rotor8.igs | 12/12/2012 | 217,161 |
| compr_rotor9.igs | 12/12/2012 | 195,048 |
| compr_stator1.igs | 12/12/2012 | 196,506 |
| compr_stator10.igs | 12/12/2012 | 171,477 |
| compr_stator2.igs | 12/12/2012 | 184,032 |
| compr_stator3.igs | 12/12/2012 | 146,448 |
| compr_stator4.igs | 12/12/2012 | 139,806 |
| compr_stator5.igs | 12/12/2012 | 118,422 |
| compr_stator6.igs | 12/12/2012 | 107,730 |
| compr_stator7.igs | 12/12/2012 | 119,637 |
| compr_stator8.igs | 12/12/2012 | 166,698 |
| compr_stator9.igs | 12/12/2012 | 148,716 |
| hub.igs | 11/30/2009 | 41,310 |
| Directory: \EEE\HPC-CR16558 Derived | | |
| blade1.igs | 12/6/2011 | 376,083 |
| blade10_cf.igs | 2/24/2012 | 311,928 |
| blade11_cf.igs | 2/24/2012 | 308,730 |
| blade12.igs | 12/6/2011 | 376,083 |
| blade13_cf.igs | 2/24/2012 | 304,958 |
| blade14.igs | 12/6/2011 | 376,083 |
| blade15.igs | 12/6/2011 | 376,083 |
| blade16.igs | 12/6/2011 | 376,083 |
| blade17.igs | 12/6/2011 | 376,083 |
| blade18_cf.igs | 3/23/2012 | 306,352 |
| blade19_cf.igs | 4/4/2012 | 312,256 |

TABLE 3.—LISTING OF FILES BY FOLDER CONTAINED IN SUPPLEMENTAL DVD

| File Name | Date Modified | Size (bytes) |
|---|---|---|
| blade2.igs | 12/6/2011 | 376,083 |
| blade20_cf.igs | 4/4/2012 | 308,402 |
| blade21_cf.igs | 4/4/2012 | 311,354 |
| blade3.igs | 12/6/2011 | 343,845 |
| blade4.igs | 12/6/2011 | 376,083 |
| blade5_cf.igs | 2/24/2012 | 306,844 |
| blade6.igs | 12/6/2011 | 376,083 |
| blade7.igs | 12/6/2011 | 376,083 |
| blade8.igs | 12/6/2011 | 376,083 |
| blade9.igs | 12/6/2011 | 376,083 |
| case.igs | 11/30/2009 | 41,310 |
| hub.igs | 11/30/2009 | 41,310 |
| README.txt | 12/19/2012 | 593 |
| Directory: \EEE\HPT | | |
| case.igs | 3/17/2010 | 21,402 |
| hpt_rotor1.igs | 12/12/2012 | 118,422 |
| hpt_rotor2.igs | 12/12/2012 | 113,967 |
| hpt_stator1.igs | 12/12/2012 | 116,640 |
| hpt_stator2.igs | 12/12/2012 | 107,568 |
| hub.igs | 3/17/2010 | 21,402 |
| Directory: \EEE\LPC | | |
| booster_rtr.igs | 12/12/2012 | 270,135 |
| booster_stator.igs | 12/12/2012 | 607,338 |
| Bypass_Outer.igs | 3/23/2010 | 34,932 |
| bypass_stator.igs | 12/12/2012 | 644,112 |
| core_guide_vane.igs | 12/12/2012 | 402,327 |
| fan.igs | 12/14/2012 | 944,541 |
| hub.igs | 3/16/2010 | 22,468 |
| LPC_bypass_hub.igs | 3/25/2010 | 14,094 |
| part_span_shroud_lower.igs | 3/16/2010 | 6,068 |
| part_span_shroud_upper.igs | 3/16/2010 | 6,068 |
| splitter_lower.igs | 3/16/2010 | 21,238 |
| splitter_upper.igs | 3/16/2010 | 21,238 |
| Directory: \EEE\LPT | | |
| case.igs | 3/17/2010 | 50,102 |
| hub.igs | 3/17/2010 | 50,102 |
| lpt_rotor1.igs | 12/12/2012 | 104,490 |
| lpt_rotor2.igs | 12/12/2012 | 103,761 |
| lpt_rotor3.igs | 12/12/2012 | 101,736 |
| lpt_rotor4.igs | 12/12/2012 | 103,923 |
| lpt_rotor5.igs | 12/12/2012 | 103,923 |
| lpt_stator1.igs | 12/12/2012 | 98,253 |
| lpt_stator2.igs | 12/12/2012 | 100,926 |
| lpt_stator3.igs | 12/12/2012 | 99,954 |
| lpt_stator4.igs | 12/14/2012 | 97,848 |
| lpt_stator5.igs | 12/12/2012 | 94,932 |

# Appendix B

Table 4 lists circumferential blade counts for the various turbomachinery components of the EEE.

TABLE 4.—CIRCUMFRENTIAL BLADE COUNT FOR EACH BLADE ROW

| LPC Blade | Count | | HPC Blade | Count | HPT Blade | Count | LPT Blade | Count |
|---|---|---|---|---|---|---|---|---|
| 1 | 32 | | 1 | 32 | 1 | 46 | 1 | 72 |
| 2 | 60 | | 2 | 28 | 2 | 76 | 2 | 120 |
| 3 | 56 | | 3 | 50 | 3 | 48 | 3 | 102 |
| 4 | 64 | | 4 | 38 | 4 | 70 | 4 | 122 |
| 5 | 34 | | 5 | 50 | | | 5 | 96 |
| | | | 6 | 68 | | | 6 | 122 |
| | | | 7 | 82 | | | 7 | 114 |
| | | | 8 | 60 | | | 8 | 156 |
| | | | 9 | 92 | | | 9 | 120 |
| | | | 10 | 70 | | | 10 | 110 |
| | | | 11 | 110 | | | | |
| | | | 12 | 80 | | | | |
| | | | 13 | 120 | | | | |
| | | | 14 | 82 | | | | |
| | | | 15 | 112 | | | | |
| | | | 16 | 84 | | | | |
| | | | 17 | 104 | | | | |
| | | | 18 | 88 | | | | |
| | | | 19 | 118 | | | | |
| | | | 20 | 96 | | | | |
| | | | 21 | 140 | | | | |

# Appendix C

Figure 7 to Figure 28 document the difference between geometry-specified leading and trailing edges for all blades of the HPC. The blades labeled UC were developed by Turner and Kiran. The Allison shapes trace back to the original CAD drawings.
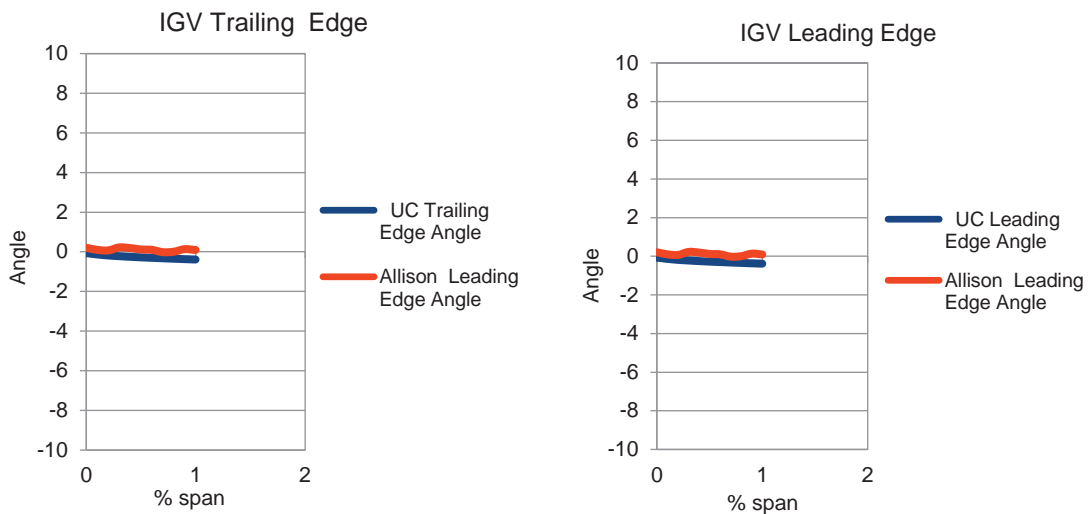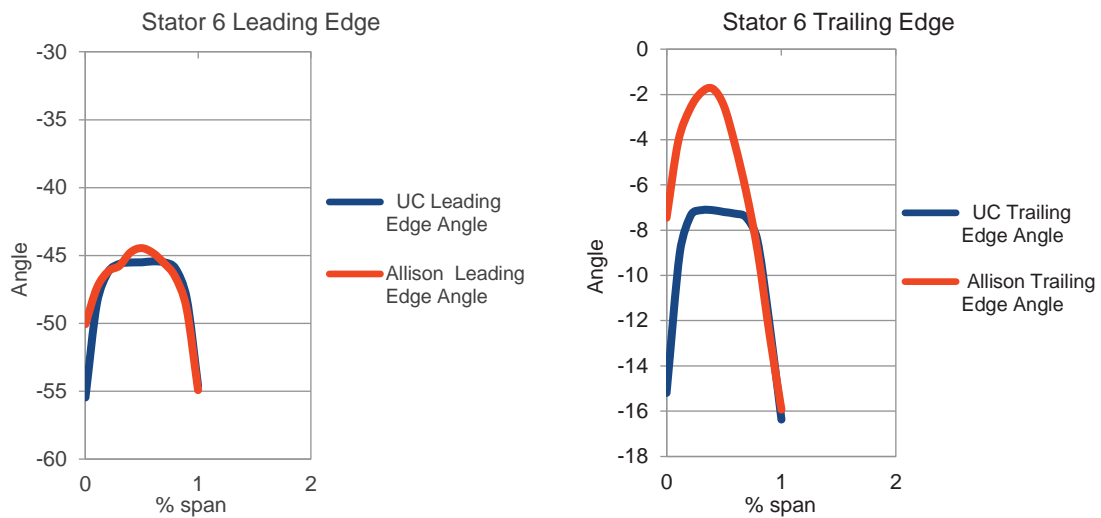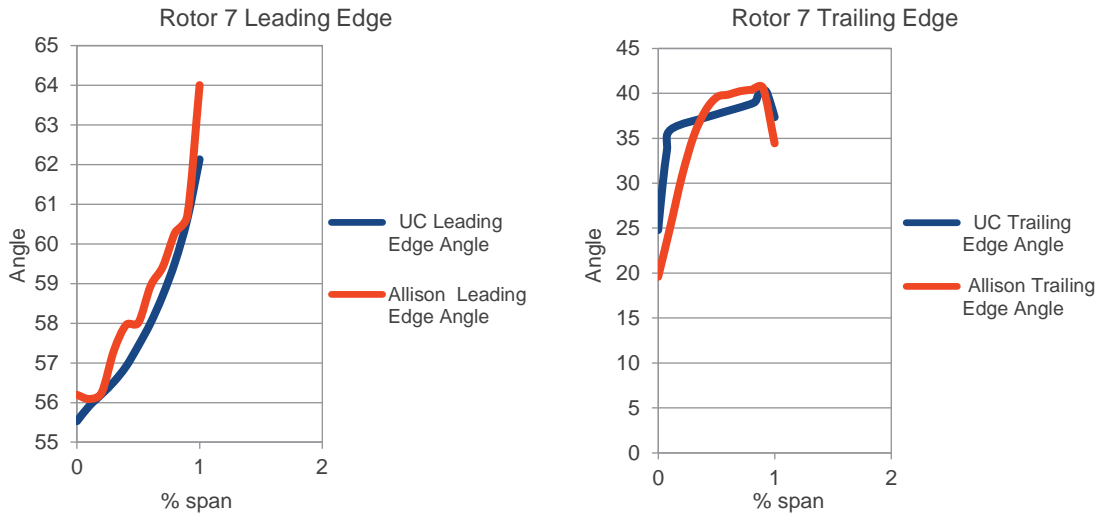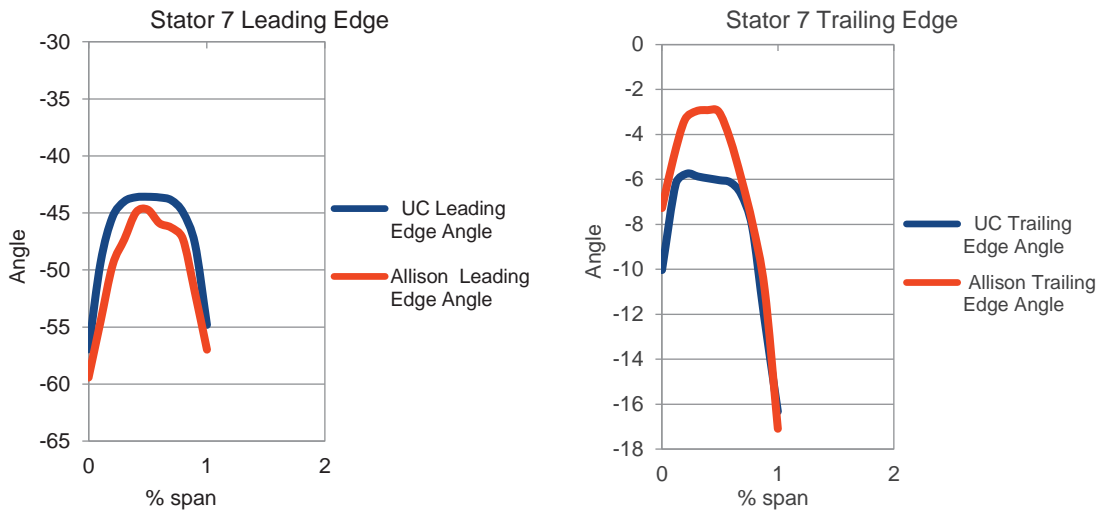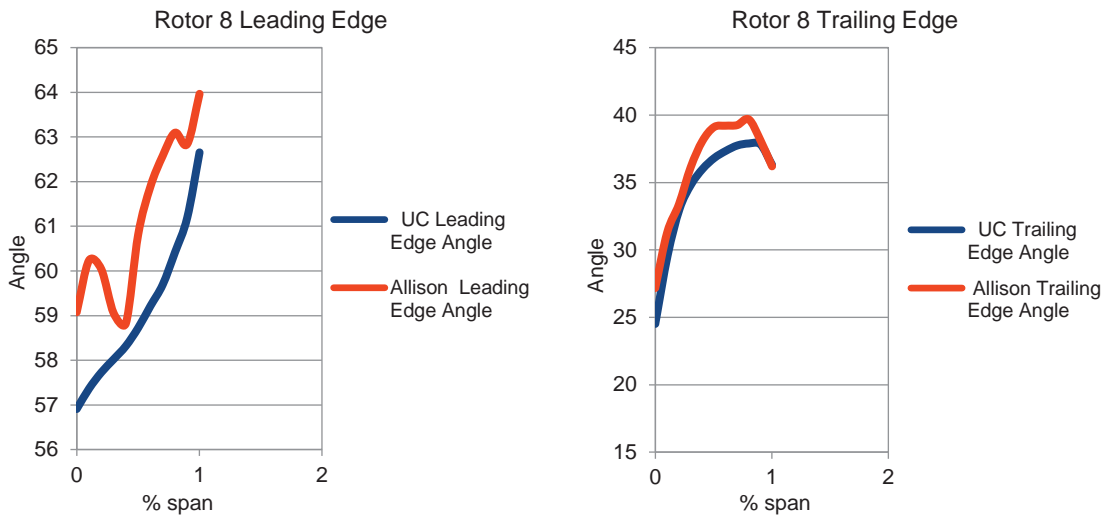


Figure 7.—Comparison of the trailing and leading edge of the IGV.
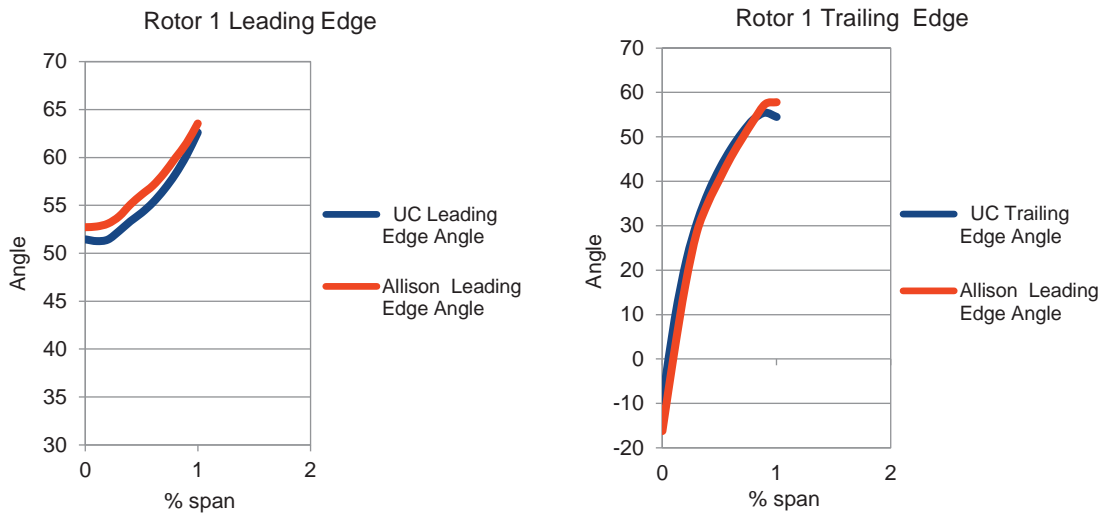
Figure 8.—Comparison of the trailing and leading edge of Rotor 1.
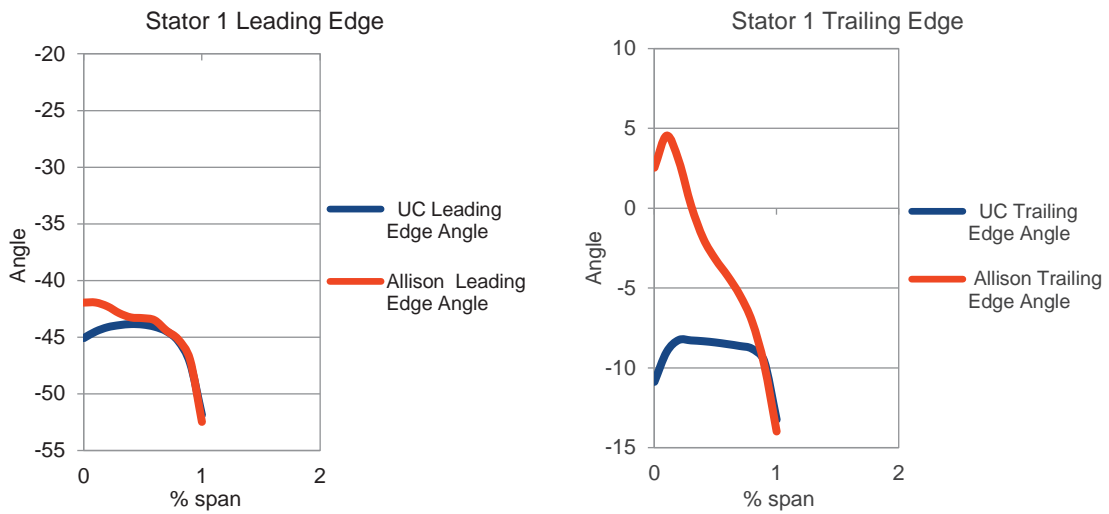


Figure 9.—Comparison of the trailing and leading edge of Stator 1.
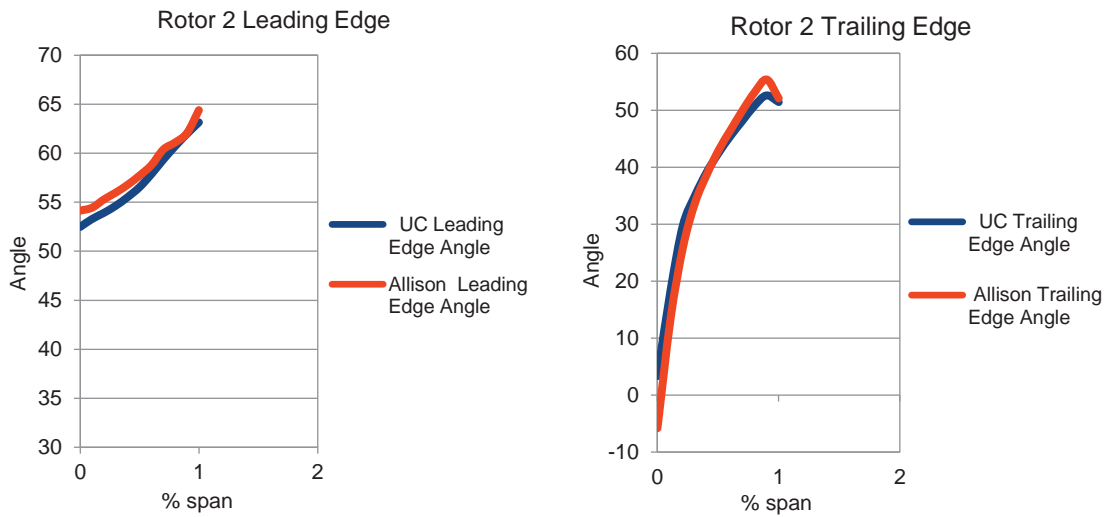
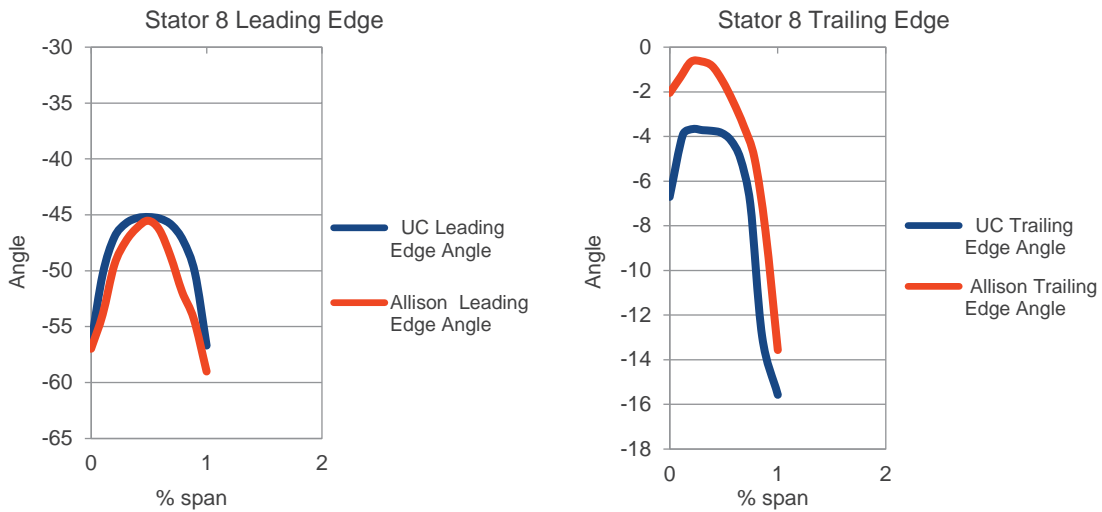Figure 10.—Comparison of the trailing and leading edge of Rotor 2.
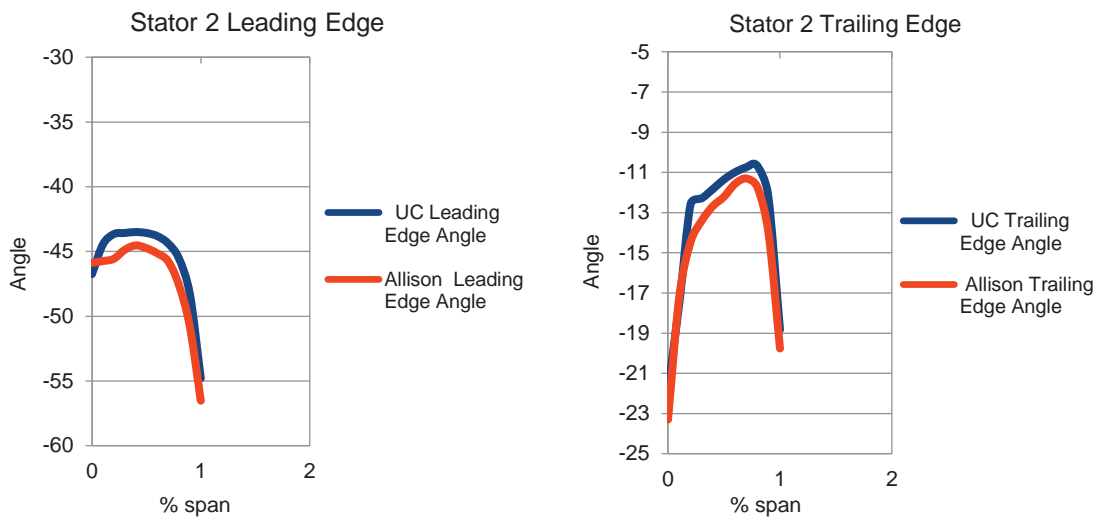


Figure 11.—Comparison of the trailing and leading edge of Stator 2.
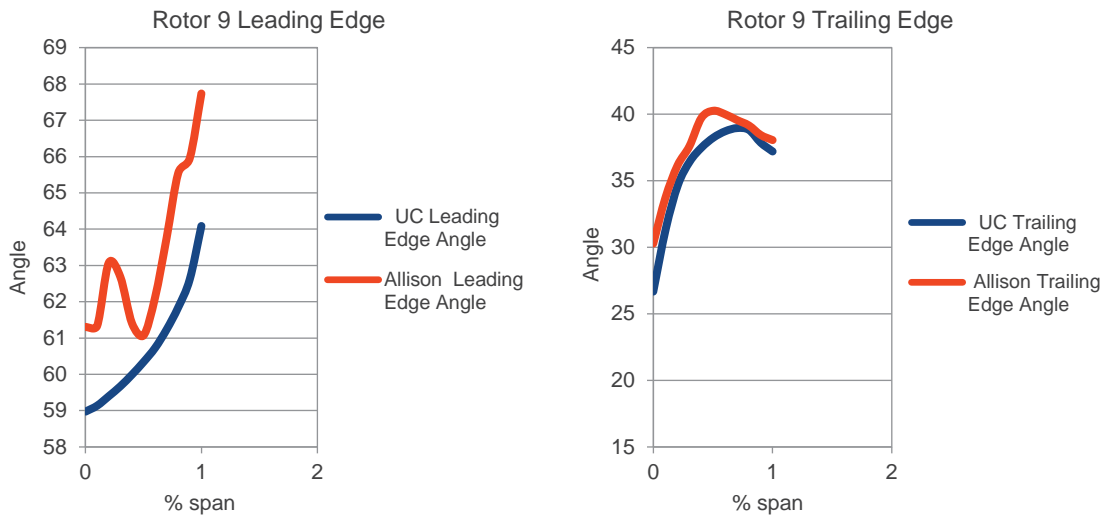
15
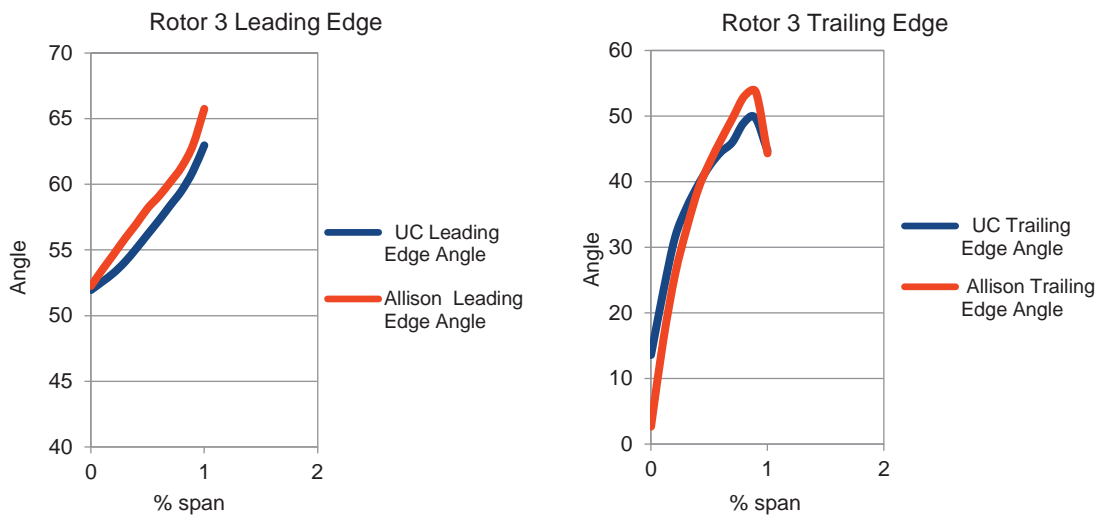
Figure 12.—Comparison of the trailing and leading edge of Rotor 3.
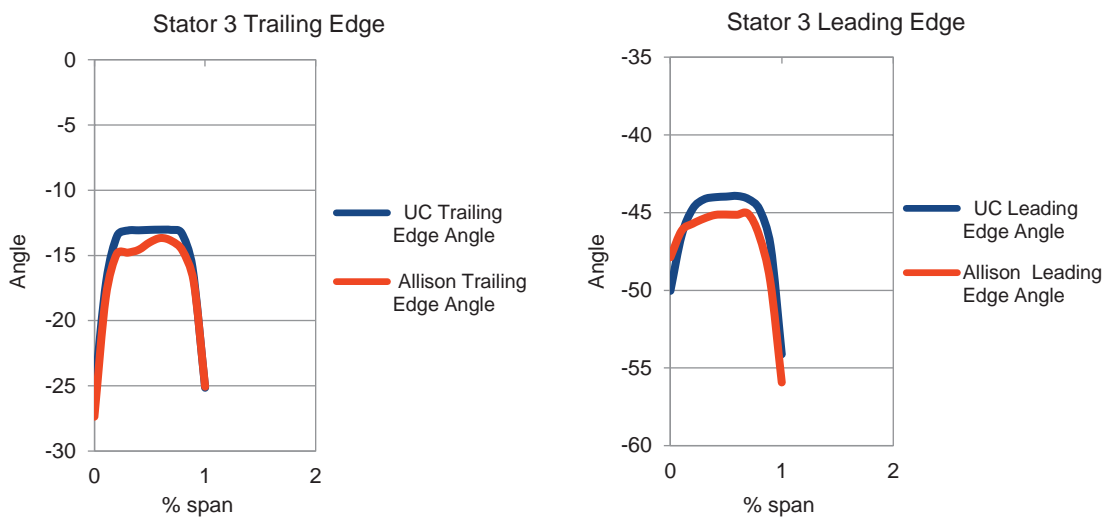


Figure 13.—Comparison of the trailing and leading edge of Stator 3.
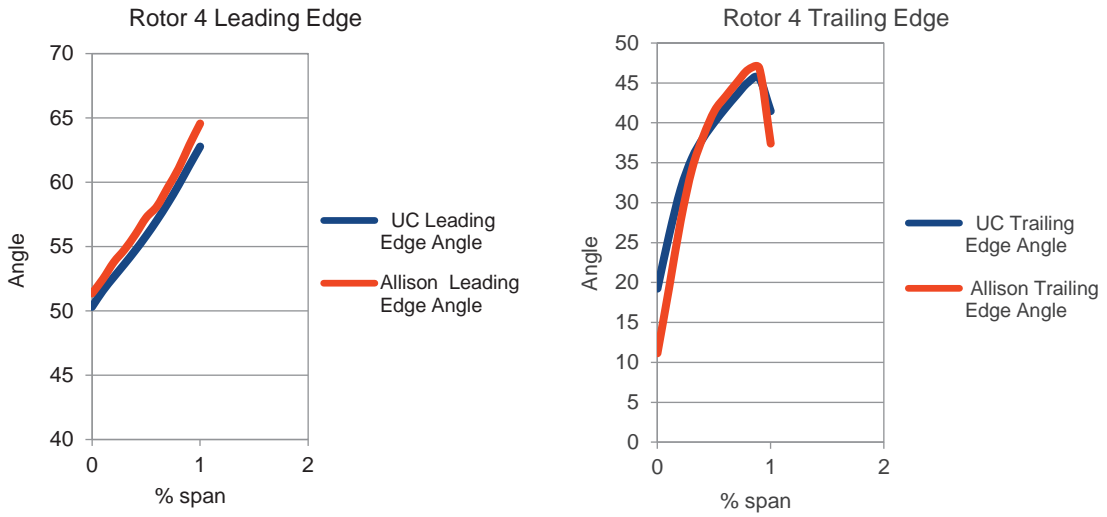
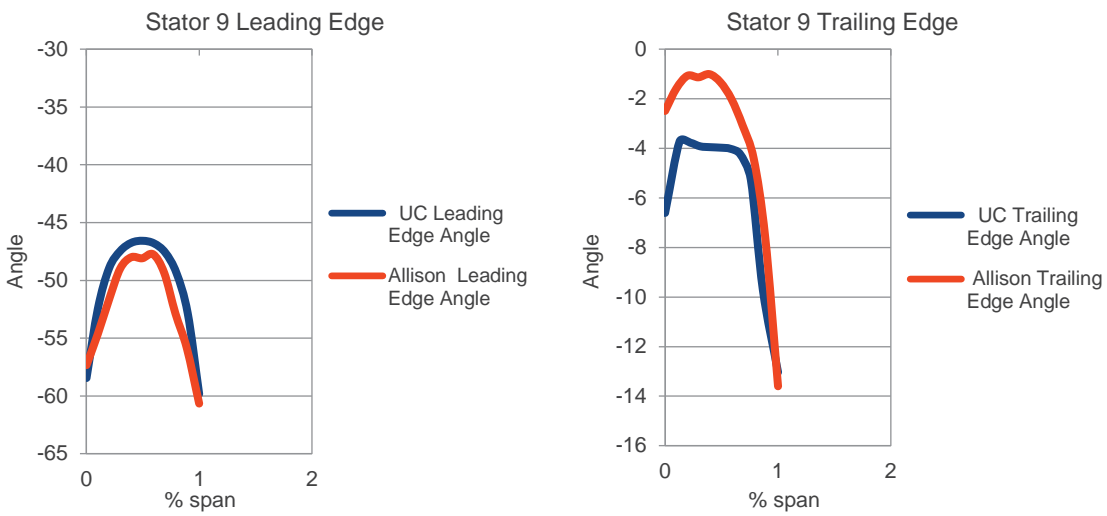Figure 14.—Comparison of the trailing and leading edge of Rotor 4.
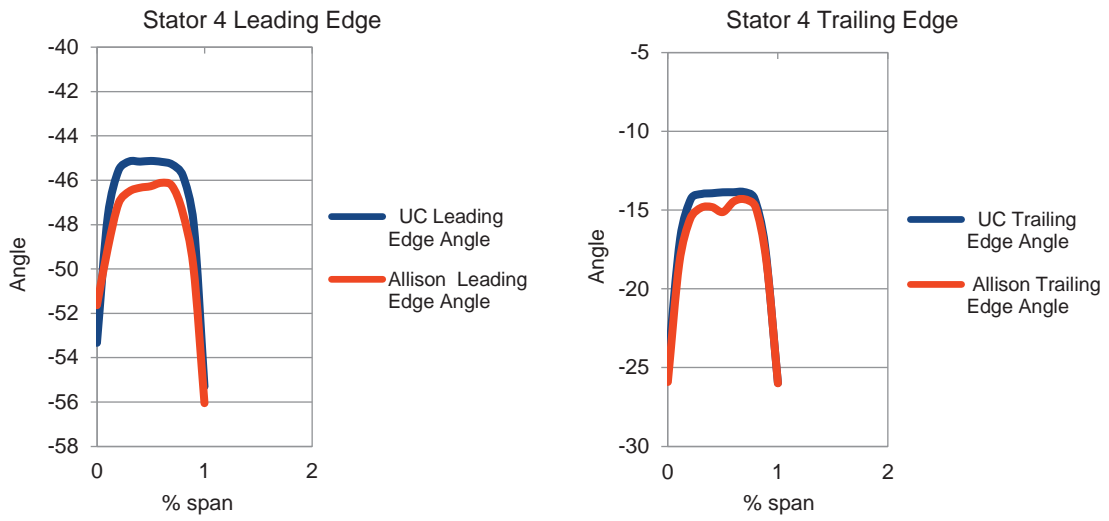


Figure 15.—Comparison of the trailing and leading edge of Rotor 4.
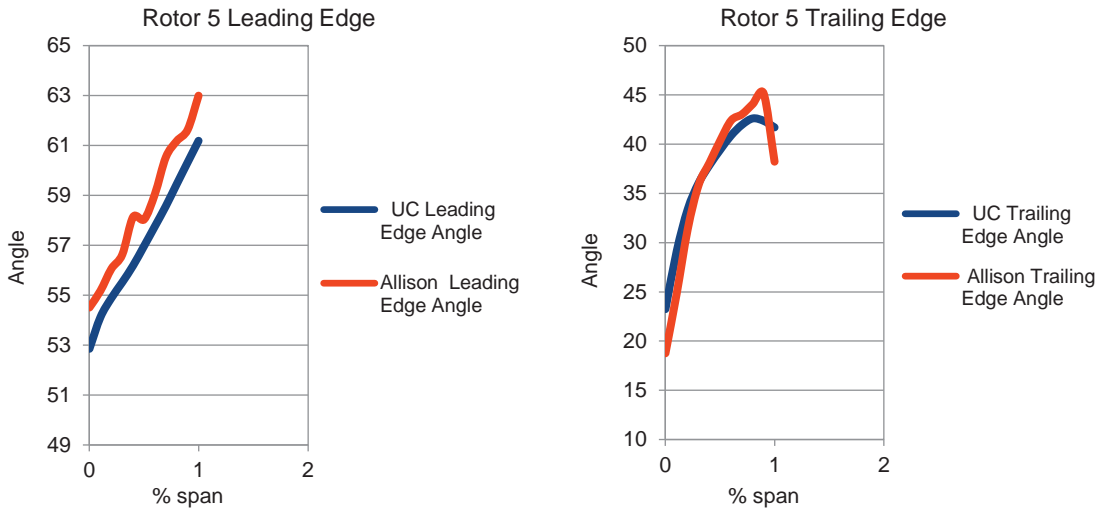
Figure 16.—Comparison of the trailing and leading edge of Rotor 5.
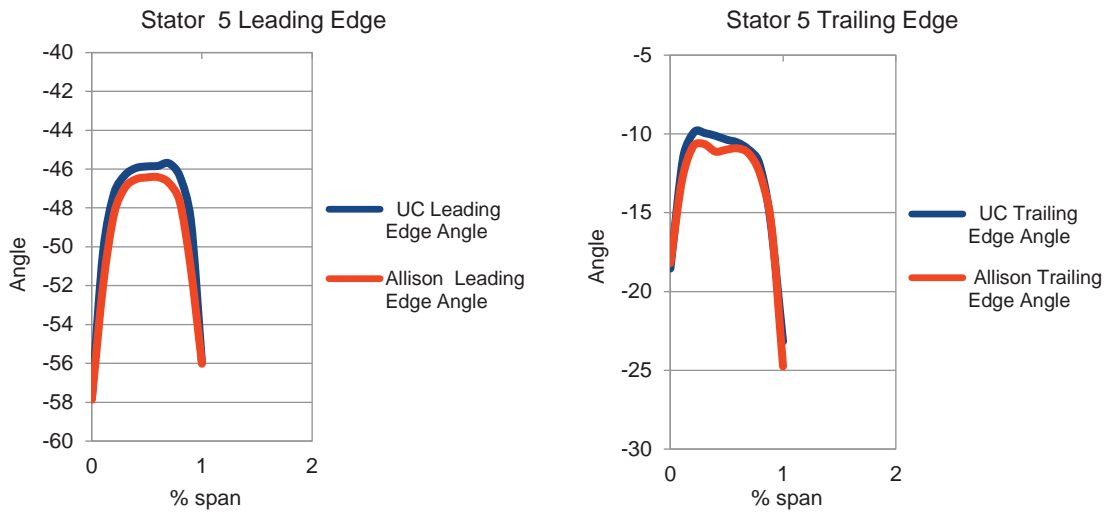


Figure 17.—Comparison of the trailing and leading edge of Stator 5.

## Rotor 6 Leading Edge



## Rotor 6 Trailing Edge
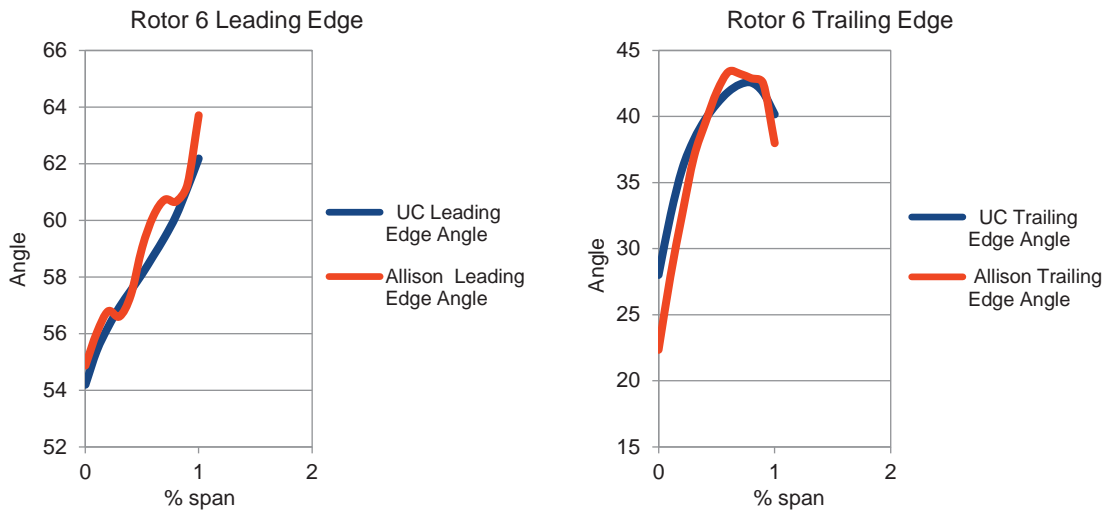


Figure 18.—Comparison of the trailing and leading edge of Rotor 6.

## Stator 6 Leading Edge



## Stator 6 Trailing Edge



Figure 19.—Comparison of the trailing and leading edge of Stator 6.

Figure 20.—Comparison of the trailing and leading edge of Rotor 7.



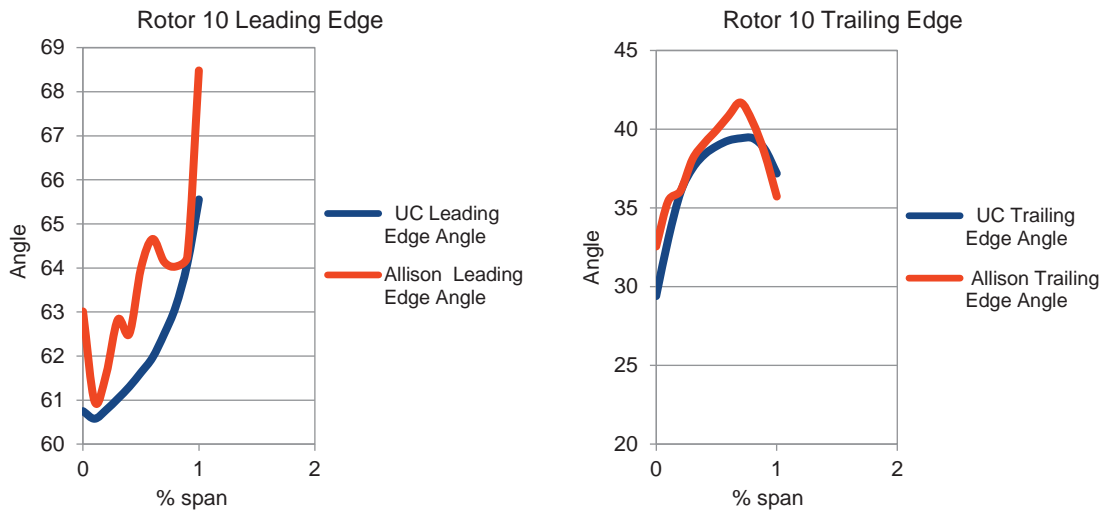Figure 21.—Comparison of the trailing and leading edge of Stator 7.

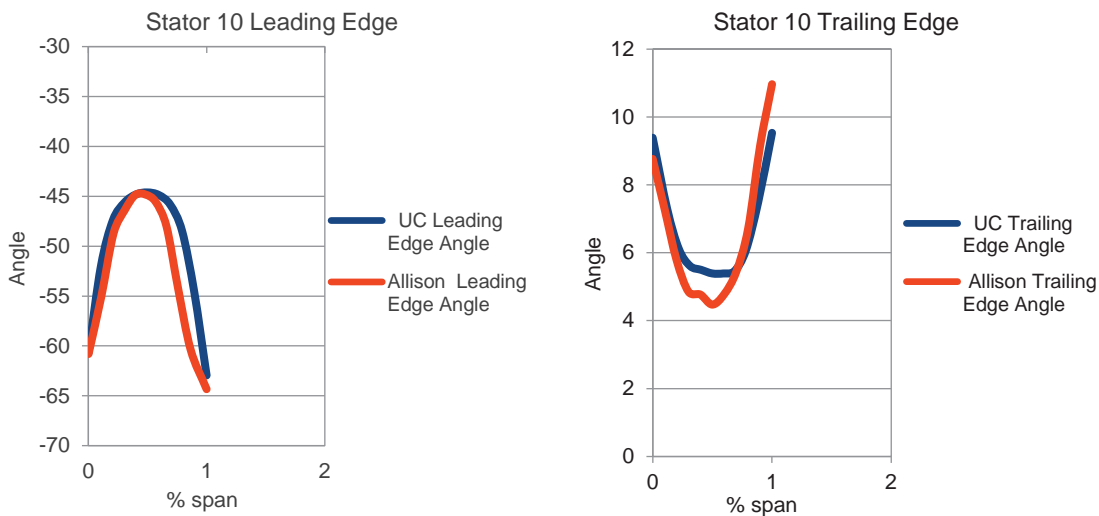Figure 22.—Comparison of the trailing and leading edge of Rotor 8.



Figure 23.—Comparison of the trailing and leading edge of Stator 8.

Figure 24.—Comparison of the trailing and leading edge of Rotor 9.



Figure 25.—Comparison of the trailing and leading edge of Stator 9.

Figure 26.—Comparison of the trailing and leading edge of Rotor 10.



Figure 27.—Comparison of the trailing and leading edge of Stator 10.

# References

1. Claus, R.W., Evans, A.L., Lytle, J.K., Nichols, L.D., "Numerical Propulsion System Simulation," Computing Systems in Engineering, Vol. 2, No. 4, pp. 357-364, 1991.
2. Claus, R.W., Townsend, S., "A Review of High Fidelity Gas Turbine Engine Simulations," ICAS 2010-475, Sept. 2010.
3. Turner, M.G., Reed, J.A., Ryder, R. and Veres, J.P., "Multi-Fidelity Simulation of a Turbofan Engine with Results Zoomed into Mini-Maps for a Zero-D Cycle Simulation," ASME Paper No. GT2004-53956, Vienna, Austria, June 2004 (also NASA/TM—2004-213076).
4. Hall, E., Owen, P., "Energy Efficient Engine HP/LP Spool Analysis," To Be Published.
5. Cline, S.J., Kutney, J.T., Halter, P.H., Sulivan, T.J., "Energy Efficient Engine Fan and Quarter-Stage Component Performance Report," NASA CR-168070, Jan. 1983.
6. Holloway, P.R., Knight, G.L., Koch, C.C., Shaffer, S.J., "Energy Efficient Engine High Pressure Compressor Detail Design Report," NASA CR-165558, May 1982.
7. Timko, L.P., " Energy Efficient Engine High Pressure Turbine Component Test Performance Report," NASA CR-168289.
8. Hall, E., Delaney, R., Lynn, S., and Veres, J. "Energy Efficient Engine Low Pressure Subsystem Aerodynamic Analysis," NASA/TM—1998-208402.
9. Hall, E., "Modular Multi-Fidelity Simulation Methodology for Multiple Spool Turbofan Engines," NASA High Performance Computing and Communications Computational Aerosciences Workshop, NASA Ames Research Center, February 15-17, 2000.
10. Stearns, EM, et al, "Energy Efficient Engine Integrated Core/Low Spool Design and Performance Report," NASA CR-168211, 1985.
11. Bridgeman, M.J., Cherry, D.G., Pedersen, J., "NASA /GE Energy Efficient Engine Low Pressure Turbine Scaled Test Vehicle Performance Test," NASA CR-168290, July 1983.
12. Vilmin, S., Lorrain, E., Hirsch, CH., Swoboda, M., "Unsteady Flow Modeling Across the Rotor / Stator Interface Using the Nonlinear Harmonic Method," ASME GT2006-90210.